



Synthesis, crystal structures and spectral characterization of imidazo [1,2-*a*]pyrimidin-2-yl-acetic acid and related analog with imidazo[2,1-*b*]thiazole ring



Agnieszka Dylong^a, Waldemar Goldman^a, Michał Sowa^a, Katarzyna Ślepokura^b, Piotr Drożdżewski^a, Ewa Matczak-Jon^{a,*}

^a Department of Chemistry, Wrocław University of Technology, Wybrzeże Wyspiańskiego 27, 50-370 Wrocław, Poland

^b Faculty of Chemistry, University of Wrocław, Joliot-Curie 14, 50-383 Wrocław, Poland

ARTICLE INFO

Article history:

Received 8 January 2016
Received in revised form
16 March 2016
Accepted 16 March 2016
Available online 19 March 2016

Keywords:

Imidazo[1,2-*a*]pyrimidine
Imidazo[2,1-*b*]thiazole
Single-crystal X-ray diffraction
Hirshfeld surface analysis
DFT calculations
Vibrational spectroscopy

ABSTRACT

Imidazo[1,2-*a*]pyrimidin-2-yl-acetic acid (*HIPM-2-ac*) and its analog with imidazo[2,1-*b*]thiazole ring (*HITZ-6-ac*) were synthesized and structurally characterized by single-crystal X-ray diffraction corroborated with calculations of Hirshfeld surfaces, which provided detailed insight into intermolecular interactions constituting both crystals.

The IR and Raman spectra of *HIPM-2-ac* and *HITZ-6-ac* were recorded and interpreted in details with the aid of Density Functional Theory (DFT) calculations and Potential Energy Distribution (PED) analysis of computed normal vibrations. Special attention was paid on hydroxyl and methylene groups involved in hydrogen bonds, which vibrations were monitored by H/D substitution. Recrystallization of parent compounds from deuterium oxide (D₂O) solutions resulted in deuteration of their carboxylic OH groups and almost complete deuteration of *HIPM-2-ac* methylene group. The latter phenomenon is clearly reflected in the vibrational spectra and confirmed by ¹H NMR experiments in solution.

© 2016 Elsevier B.V. All rights reserved.

1. Introduction

Synthetic heterocycles constitute a vast family of compounds gaining substantial interest in the field of medicinal chemistry. Their great pharmacological potential lies in structural similarity to naturally occurring heterocycles such as purines or indoles, which makes them capable of binding to multiple biological targets with high affinity and providing pharmaceutical activities in diverse cellular processes. Of significant interest are bicyclic systems containing imidazole ring, which is a common motif encountered in biologically active compounds produced by nature [1–5]. Among them imidazo[1,2-*a*]pyridine (IP) is the most widely studied and most frequently represented in marketed drug formulations [2]. Scientific interest is also related to synthesis and evaluation of biological activities of the compounds containing imidazo[1,2-*a*]pyrimidine (IPM) and imidazo[2,1-*b*]thiazole (ITZ) scaffolds. Numerous members of IPM and ITZ families have been reported to exhibit remarkable potential as anxiolytic [6], antimicrobial [7],

antiparasitic [8], antiviral [9] or anticancer [10] agents.

Pharmaceutical significance of the compounds containing fused IP, IPM and ITZ heterocyclic rings and limited literature available regarding their structural and physicochemical characterization are two important factors that prompted us to initiate systematic studies on imidazole-based bicyclic systems appended with acetic group. Recently, we have demonstrated that imidazo[1,2-*a*]pyrimidin-2-yl-acetic acid (*HIP-2-ac*) exists in the solid state as a zwitterion, with a proton transferred from carboxylic group to imidazole N atom and acts as a bifunctional N,O-donor ligand forming mostly mononuclear complexes with d block metal ions [11,12]. In continuation of our research interest in this class of compounds, herein we report the synthesis, crystal structures and detailed vibrational characterization of two structurally similar compounds, namely, imidazo[1,2-*a*]pyrimidin-2-yl-acetic acid (*HIPM-2-ac*, **1**) and imidazo[2,1-*b*]thiazol-6-yl-acetic acid (*HITZ-6-ac*, **2**) which has been previously reported to be moderate anti-inflammatory agent [13].

Single crystal X-ray diffraction studies have revealed that **1** and **2** crystallize as electrically neutral molecules, which is in contrast to previously reported *HIP-2-ac* [11]. The structural descriptions have

* Corresponding author.

E-mail address: ewa.matczak-jon@pwr.edu.pl (E. Matczak-Jon).

additionally been corroborated with calculations of Hirshfeld surfaces, which provide detailed insight into intermolecular interactions constituting crystals **1** and **2**. Experimental IR and Raman spectra of both compounds and their deuterated isotopologues **1a** and **2a** have been interpreted in details with the aid of DFT calculations and PED analysis of computed normal vibrations. Moreover, H/D substitution spectral effects have been used for respective band assignments. As expected, typical three-fold recrystallization of **2** from D₂O/CD₃OD solutions resulted in almost complete deuteration of its carboxylic OH group. Surprisingly, in case of **1** both carboxylic and methylene groups have been found to be deuterated. A rare phenomenon of H/D exchange in methylene group of **1** has been revealed based on analysis of vibrational spectra of **1** and **1a**. A further support has been provided by ¹H NMR spectra of D₂O solutions of **1** and **2** recorded as a function of time. The spectra of **1** have demonstrated gradual decrease in intensity of methylene group signal followed by its disappearance after c.a. three days. In contrast, only insignificant spectral changes have been observed under similar conditions for **2**.

2. Experimental

2.1. General information and materials

All reagents were obtained from commercial sources and used without further purification.

2.2. Syntheses of the compounds **1** and **2** and their precursors

Ethyl imidazo[2,1-*b*]thiazol-6-yl-acetate: in an 1000 ml round-bottomed flask, a mixture of 45.0 g (0.215 mol) of the crude, freshly prepared ethyl 4-bromoacetate [14], 25.2 g (0.30 mol) of the sodium bicarbonate and 20.0 g (0.20 mol) of 2-aminothiazole in mixture of 400 ml 1,4-dioxane and 200 ml of anhydrous ethanol was vigorously stirred for 16 h at room temperature and refluxed for 8 h. The crude reaction mixture was evaporated to dryness and 400 ml of water was added. The water solution was extracted with dichloromethane (2 × 150 ml) and the organic extracts were washed with saturated solution of NaHCO₃ (2 × 200 ml). The organic layer was dried over anhydrous Na₂SO₄, filtered through a plug of silica gel (30 g) and the filtrate was extracted with 1 M HCl_{aq} (5 × 150 ml). The combined aqueous phases were neutralized with solid sodium bicarbonate, extracted with dichloromethane (2 × 150 ml), dried over anhydrous Na₂SO₄ and concentrated under reduced pressure to afford a crude ethyl imidazo[2,1-*b*]thiazol-6-yl-acetate (28.5 g, 68% yield) as a light brown thick liquid.

¹H NMR (CDCl₃, 300 MHz): δ = 1.26 (t, *J* = 7.1 Hz, 3H, CH₃), 3.72 (s, 2H, CH₂), 4.16 (quartet, *J* = 7.1 Hz, 2H, OCH₂), 6.76 (d, *J* = 4.6 Hz, 1H, H-2), 7.34 (d, *J* = 4.6 Hz, 1H, H-3), 7.41 (s, 1H, H-5) ppm. ¹³C NMR (CDCl₃, 75 MHz): δ = 14.08 (s, CH₃), 35.10 (CH₂), 60.79 (OCH₂), 110.81 (C-2), 111.92 (C-5), 118.54 (C-3), 140.66 (C-6), 149.08 (C-8), 170.80 (COO) ppm. The ¹H and ¹³C NMR spectra are in agreement with those described in the literature [13].

Ethyl imidazo[1,2-*a*]pyrimidin-2-yl-acetate was synthesized from 19.0 g (0.20 mol) of 2-aminopyrimidine by the procedure used for ethyl imidazo[2,1-*b*]thiazol-6-yl-acetate (300 ml of anhydrous ethanol was used as solvent). Ethyl imidazo[1,2-*a*]pyrimidin-2-yl-acetate was obtained as brown thick oil (4.5 g, 11% yield), which solidified upon standing at room temperature.

¹H NMR (CDCl₃, 300 MHz): δ = 1.27 (t, *J* = 7.2 Hz, 3H, CH₃), 3.90 (s, 2H, CH₂), 4.18 (quartet, *J* = 7.2 Hz, 2H, OCH₂), 6.82 (dd, *J* = 6.7 Hz, *J* = 4.1 Hz, 1H, H-6), 7.58 (s, 1H, H-3), 8.38 (dd, *J* = 6.7 Hz, *J* = 2.1 Hz, 1H, H-5), 8.48 (dd, *J* = 4.1 Hz, *J* = 2.1 Hz, 1H, H-7) ppm. ¹³C NMR (CDCl₃, 75 MHz): δ = 14.21 (s, CH₃), 35.32 (CH₂), 61.13 (OCH₂), 109.18 (C-6), 111.64 (C-3), 133.11 (C-5), 141.87 (C-2), 147.98 (C-9),

149.74 (C-7), 170.57 (COO) ppm.

The ¹H and ¹³C NMR signal assignments were performed on the basis of literature data [15,16].

Imidazo[1,2-*a*]pyrimidin-2-yl-acetic acid (1**) and imidazo[2,1-*b*]thiazol-6-yl-acetic acid (**2**)**. To solution of the respective crude ethyl ester (0.02 mol) in 100 ml of methanol 1.1 g (0.028 mol) of NaOH was added, resulted mixture was refluxed for 4 h and cooled to room temperature. 12 M hydrochloric acid was added dropwise (~2.3 ml, 0.028 mol), the mixture was concentrated under reduced pressure and the residue was treated with 30 ml of diethyl ether. The solid was filtered by suction and washed with 15 ml portions of diethyl ether (until the filtrates became colorless). The resulted solid still containing sodium chloride was dried under reduced pressure, dissolved in about 100 ml of boiling water, decolorized with activated charcoal and concentrated to 25–30 ml. The solution was left for 24 h at room temperature, the crystallized solid was filtered by suction and washed with cold water (3 × 5 ml) and acetone (2 × 25 ml). That gave 1.5 g (43%) of imidazo[1,2-*a*]pyrimidin-2-yl-acetic acid (**1**) as beige powder and 1.5 g (41%) of imidazo[2,1-*b*]thiazol-6-yl-acetic acid (**2**) as the white tiny needles.

Imidazo[1,2-*a*]pyrimidin-2-yl-acetic acid (1**)**. ¹H NMR (DMSO-*d*₆, 300 MHz): δ = 3.73 (s, 2H, CH₂), 7.00 (dd, *J* = 4.1 Hz, *J* = 6.7 Hz, 1H, H-6), 7.80 (s, 1H, H-3), 8.46 (dd, *J* = 4.1 Hz, *J* = 2.0 Hz, 1H, H-7), 8.91 (dd, *J* = 2.0 Hz, *J* = 6.7 Hz, 1H, H-5), 12.43 (broad, 1H, COOH) ppm. ¹³C NMR (DMSO-*d*₆, 75 MHz): δ = 35.35 (CH₂), 108.93 (C-6), 110.11 (C-3), 135.50 (C-5), 141.74 (C-2), 147.53 (C-9), 149.89 (C-7), 172.32 (COOH) ppm. The ¹H and ¹³C NMR signal assignments are consistent with literature data [15,16]. (For more details see Figs. S1 and S3); m.p. = 205–206 °C (H₂O), literature m.p. = 213–214 °C (EtOH) [17].

Imidazo[2,1-*b*]thiazol-6-yl-acetic acid (2**)**. ¹H NMR (DMSO-*d*₆, 300 MHz): δ = 3.56 (s, 2H, CH₂), 7.17 (d, *J* = 4.4 Hz, 1H, H-2), 7.61 (s, 1H, H-5), 7.83 (d, *J* = 4.4 Hz, 1H, H-3), 12.36 (broad, 1H, COOH) ppm. ¹³C NMR (DMSO-*d*₆, 75 MHz): δ = 35.34 (CH₂), 112.01 (C-5), 112.77 (C-2), 120.31 (C-3), 141.33 (C-6), 148.35 (C-8), 172.57 (COOH) ppm. ¹H NMR spectrum is in agreement with the literature data [13] (for more details see Figs. S2 and S4); m.p. = 180–181 °C (H₂O), literature m.p. = 185–187 °C (EtOH) [13].

Compounds **1a** and **2a** were obtained by a recrystallization of **1** and **2** from D₂O and CD₃OD, respectively.

2.3. X-ray crystallography

Crystallographic measurements were performed on a Kuma KM4-CCD automated four-circle diffractometer with graphite monochromatized Mo K α radiation at 100(2) K using an Oxford Cryosystems cooler. Data collection, cell refinement, data reduction and analysis were carried out with CRYALISCCD and CRYALISRED, respectively [18]. Multi-scan (for **1**) and analytical (for **2**) absorption correction was applied to the data with use of CRYALISRED. Both structures were solved with direct methods using SHELXS-2014 [19a] and refined by a full-matrix least squares technique with SHELXL-2014 [19b] with anisotropic thermal parameters for all non-H atoms. All H-atoms were initially located in difference Fourier maps, and in the final refinement cycles were treated as described below. All C-bound H atoms were placed in calculated positions, with C–H = 0.95–0.99 Å, and refined with a riding model with $U_{iso}(H) = 1.2U_{eq}(C)$. O-bound H atoms were allowed to refine with O–H distance restrained to 0.840(2) Å and $U_{iso}(H) = 1.5U_{eq}(O)$, and then they were constrained to ride on parent atoms (AFIX 3 instruction in SHELXL-2014). Crystallographic data and structure refinement parameters are summarized in Table 1. All figures were made using DIAMOND program [20].

Table 1
Summary of crystallographic data and structure refinement results for **1** and **2**.

Compound	1	2
CCDC No.	1436747	1436748
Formula	C ₈ H ₇ N ₃ O ₂	C ₇ H ₆ N ₂ O ₂ S
Formula weight	177.17	182.20
Crystal system	orthorhombic	orthorhombic
Space group	<i>Pca</i> 2 ₁	<i>P</i> 2 ₁ 2 ₁ 2 ₁
<i>a</i> (Å)	19.255(6)	5.482(2)
<i>b</i> (Å)	5.095(2)	7.449(3)
<i>c</i> (Å)	7.572(3)	18.038(6)
<i>V</i> (Å ³)	742.8(5)	736.6(5)
<i>Z</i>	4	4
Crystal size (mm)	0.36 × 0.25 × 0.10	0.40 × 0.24 × 0.06
Temperature (K)	100(2)	100(2)
Radiation	Mo Kα	Mo Kα
Wavelength (Å)	0.71073	0.71073
μ (mm ⁻¹)	0.12	0.39
d_{calc} (g·cm ⁻³)	1.584	1.643
<i>F</i> (000)	368	376
θ range (°)	3.4–28.7	3.0–28.6
Reflections collected	5191	5727
Reflections independent	1705	1799
Reflections observed (<i>I</i> > 2 σ (<i>I</i>))	1614	1720
<i>R</i> _{int}	0.034	0.041
Absorptions correction	Empirical (multi-scan)	Analytical
<i>T</i> _{min} / <i>T</i> _{max}	0.843/1.000	0.859/0.976
Data/parameters/restraints	1705/118/2	1799/109/1
<i>R</i> ₁ ; <i>wR</i> ₂ (<i>F</i> _o ² > 2 σ (<i>F</i> _o ²))	0.034; 0.088	0.033; 0.087
<i>R</i> ₁ ; <i>wR</i> ₂ (all data)	0.036; 0.089	0.035; 0.088
GoF = <i>S</i> _{all}	1.10	1.05
$\Delta\rho_{\text{max}}/\Delta\rho_{\text{min}}$ (eÅ ⁻³)	0.21/–0.23	0.33/–0.28
Absolute structure parameter	–	0.00(5)

2.4. Hirshfeld surface analysis

Hirshfeld surface maps and 2D fingerprint plots were prepared using Crystal-Explorer v.3.0 [21] enabling quantitative estimation of percentage contributions for various intermolecular contacts in the reported crystals of **1** and **2**.

2.5. Spectroscopy

Room-temperature 1D (¹H, ¹³C NMR) spectra of **1** and **2** dissolved in DMSO-*d*₆ were obtained using Bruker DRX 300 MHz spectrometer operating at 300.13 and 75.46 MHz for ¹H and ¹³C, respectively. All remaining experiments were performed using Bruker Avance™ 600 MHz spectrometer operating at 600.13 MHz for ¹H and 150.90 MHz for ¹³C. The standard Bruker program was used to perform HSQC correlation experiments confirming spectral assignments of **1** and **2**. All experiments were performed with locking spectrometer on deuterium from a solvent. Chemical shifts are given in relation to TMS (SiMe₄). All downfield shifts are denoted as positive.

Infrared (ATR FT-IR) spectra were measured on a Bruker Vertex 70v Fourier transform infrared spectrometer equipped with a diamond ATR cell. The spectral data were collected as 64 scans at room temperature over the range 4000–400 cm⁻¹ and 600–40 cm⁻¹ with a resolution of 4 and 2 cm⁻¹, respectively.

Raman spectra were collected on a Bruker MultiRam FT spectrometer equipped with a liquid nitrogen cooled germanium detector and Nd:YAG laser with emitting radiation at a wavelength of 1064 nm. For each sample 128 scans were accumulated at laser power equal 450 mW and with a resolution of 2 cm⁻¹.

For IR and Raman measurements, the instrument control and initial data processing were performed using OPUS software (v. 7.0 Bruker Optics, Ettlingen, Germany).

2.6. Theoretical (DFT) calculations

The DFT calculations for **1** and **2** were performed employing the GAUSSIAN 09 package [22]. The B3LYP functional [23] and LanL2DZ basis set [24] were employed for providing a good comparison with similar calculations to be carried out for metal complexes which we are preparing with present and similar ligands. The calculations of normal vibrations were performed on the optimized structures, well corresponding to these determined by single-crystal X-ray diffraction. Besides, the calculations for deuterated **1a** and **2a** isotopologues have also been performed. The potential energy distribution (PED) terms were calculated by Fcarrt66 package [25]. Normal vibrations and corresponding IR and Raman bands were characterized on the basis of PED results and additionally verified by atom displacement animation done by Chemcraft program [26]. Calculation results were converted into theoretical spectra using the Chemcraft application with Lorentzian band shape and 5 cm⁻¹ half band width. For easier comparison of observed and calculated band positions the wavenumbers calculated above 2000 cm⁻¹ were scaled by 0.96 factor, typical for applied computation method [27].

3. Results and discussion

3.1. Synthesis of **1**, **2** and their precursors

The synthesis of HIPM-2-*ac* (**1**) and HITZ-6-*ac* (**2**) is outlined in Schemes 1 and 2, respectively. Both compounds were prepared by alkaline hydrolysis of the appropriate ethyl esters following neutralization of obtained salts. Thus, crude ethyl imidazo[1,2-*a*]pyrimidin-2-yl-acetate and ethyl imidazo[2,1-*b*]thiazol-6-yl-acetate were hydrolyzed to the sodium salt with sodium hydroxide in boiling methanol and neutralized with stoichiometric amount of hydrochloric acid to desired HIPM-2-*ac* and HITZ-6-*ac*.

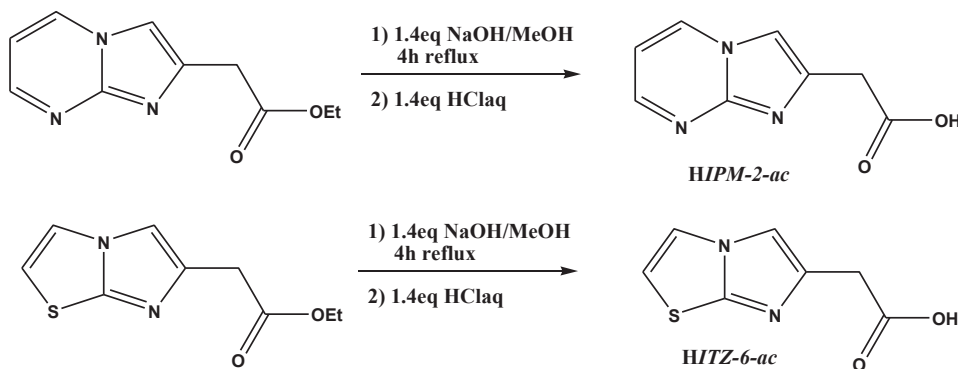
Starting ethyl esters of above ligands were prepared by the modification of the literature procedure, which is based on condensation of ethyl 4-bromoacetoacetate with 2-aminopyrimidine [17,28] and 2-aminothiazole [13,29]. The same modification was used previously for the synthesis of imidazo[1,2-*a*]pyrimidin-2-yl-acetic acid (HIP-2-*ac*) and its ethyl ester [11]. Thus, ethyl imidazo[1,2-*a*]pyrimidin-2-yl-acetate was obtained with 11% yield by the condensation of crude ethyl 4-bromoacetoacetate (prepared by bromination of the ethyl acetoacetate [14]) with 2-aminopyrimidine in the presence of sodium bicarbonate in 1,4-dioxane. Similar reaction with 2-aminothiazole in the 1,4-dioxane–ethanol mixture gave ethyl imidazo[2,1-*b*]thiazol-6-yl-acetate in 68% yield (Scheme 2).

3.2. Solid state characterization of **1** and **2**

Molecular structures and atom-numbering schemes for HIPM-2-*ac* (**1**) and HITZ-6-*ac* (**2**) are shown in Fig. 1 whereas geometrical parameters of hydrogen bonds are given in Table 2.

Compounds **1** and **2** crystallize as electrically neutral molecules in non-centrosymmetric *Pca*2₁ and *P*2₁2₁2₁ space groups of the orthorhombic crystal system, respectively. This is in contrast to previously described HIP-2-*ac* [11], which crystallizes as a zwitterion with proton transferred from carboxylic group to imidazole N atom. In both **1** and **2** the carboxylic group adopts the same orientation with respect to the plane defined by the aromatic ring and C10/C9 atoms. This is reflected in N1–C2–C10–C11 and N7–C6–C9–C10 dihedral angles of 71.1(2) and –73.1(3)°, respectively.

Crystal structures of **1** and **2** reveal presence of zig–zag tape motifs (Fig. S5) formed by hydrogen bonds between molecules related by action of a 2₁ screw axis. In **1**, those interactions comprise



Scheme 1.

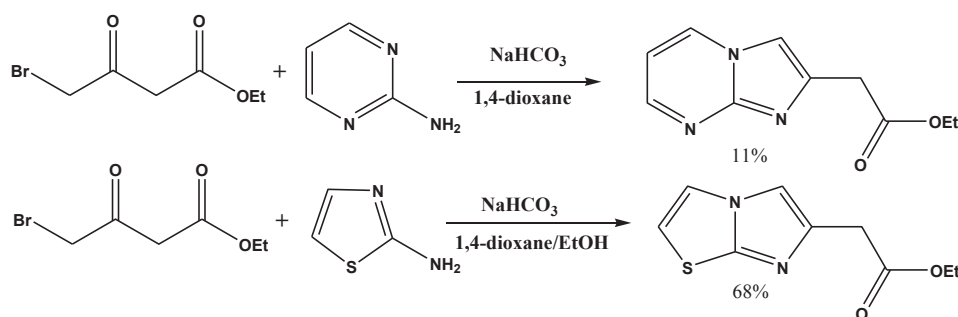
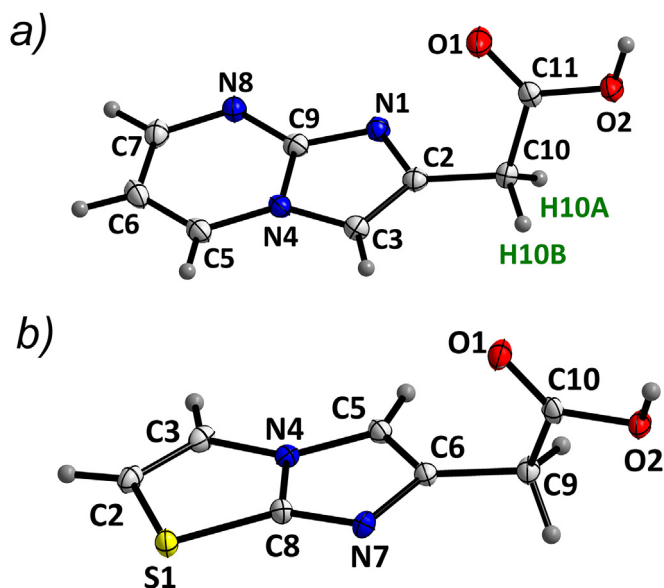
Scheme 2. Synthesis of ethyl imidazo[1,2-a]pyrimidin-2-yl-acetate and ethyl imidazo[2,1-b]thiazol-6-yl-acetate precursors of **1** and **2**.

Fig. 1. Asymmetric units of **1** (a) and **2** (b) showing atom-numbering schemes. Displacement ellipsoids are drawn at 50% probability level. (v(C–H) vibrations of methylene H atoms of **1** given in green are discussed in details in a paragraph 3.4.). (For interpretation of the references to colour in this figure legend, the reader is referred to the web version of this article).

Table 2

Geometry of proposed hydrogen bonds and close C–H···O contacts in **1** and **2**.

D–H···A	D–H	H···A	D···A	D–H···A
Compound 1				
O2–H2···N1 ⁱ	0.84	1.81	2.652(2)	178
C3–H3···O1 ⁱⁱ	0.95	2.59	3.414(3)	145
C6–H6···O2 ⁱⁱⁱ	0.95	2.53	3.261(3)	134
C7–H7···O1 ^{iv}	0.95	2.53	3.410(3)	154
C10–H10A···O1 ^v	0.99	2.41	3.176(3)	133
Compound 2				
O2–H2O···N7 ^{vi}	0.84	1.84	2.670(3)	171
C2–H2···O1 ^{vii}	0.95	2.45	3.235(3)	140
C5–H5···O1 ^{viii}	0.95	2.34	3.283(3)	172
C9–H9B···O1 ^{ix}	0.99	2.59	3.287(3)	127

Symmetry codes: (i) $-x+1, -y+1, z-1/2$; (ii) $x, y+1, z$; (iii) $x-1/2, -y+2, z$; (iv) $-x+1/2, y, z+1/2$; (v) $-x+1, -y+1, z+1/2$; (vi) $-x, y+1/2, -z+3/2$; (vii) $x+1/2, -y+3/2, -z+1$; (viii) $x+1, y, z$; (ix) $-x, y-1/2, -z+3/2$.

(symmetry codes in Table 2) form the zig–zag tapes in crystallographic *b* direction and similarly to **1**, respective R²₂(8) ring motifs are also observed.

Similar zig–zag tapes have been found in the crystal structure of previously reported HIP-2-ac [11], however in the latter case zwitterions are connected by N–H···O and C–H···O interactions. Stabilization of the three-dimensional crystal lattices in **1** and **2** is provided by C–H···O-type contacts between neighboring zig–zag tapes (Figs. 2 and 3, Table 2).

3.3. Hirshfeld surface analysis

Inspection of corresponding Hirshfeld surfaces can provide an additional, qualitative and quantitative insight into similarities and differences between interactions in the two reported herein compounds.

O2–H2···N1ⁱ and C10–H10A···O1^v contacts (symmetry codes in Table 2) stabilizing the zig–zag motif in the crystallographic *c* direction. The above mentioned interactions lead to formation of ring motifs that can be described by R²₂(8) graph set notation [30]. In **2**, corresponding O2–H2O···N7^{vi} and C9–H9B···O1^{ix} interactions

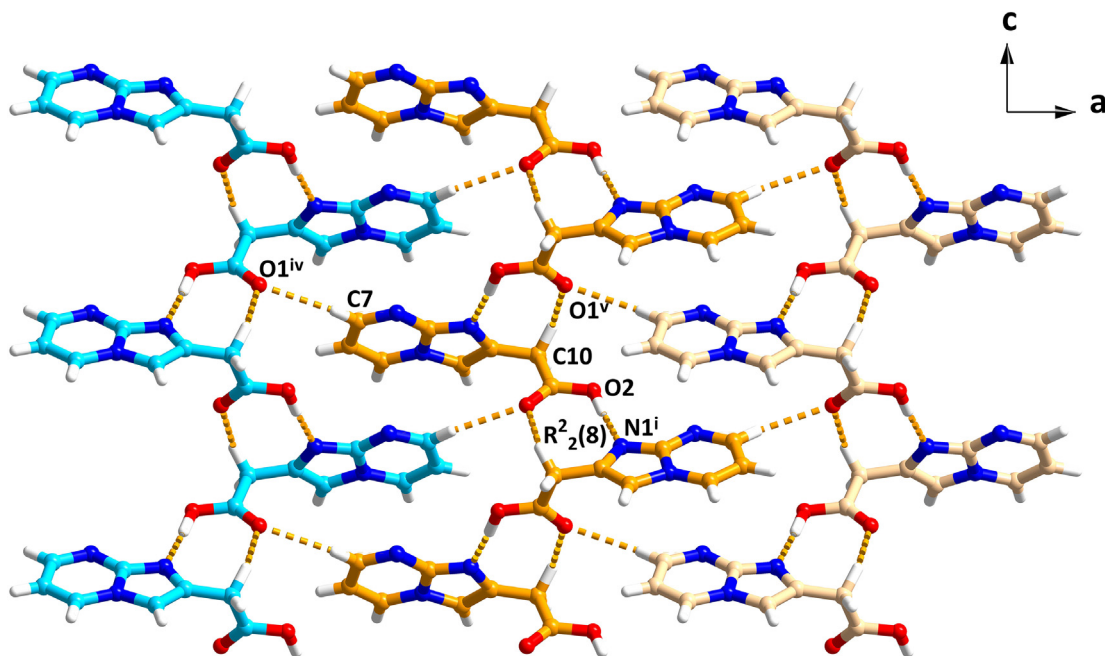


Fig. 2. A packing diagram for **1** showing selected C–H···O interactions between neighbouring zig–zag tapes (shown in blue, orange and tan) in the crystallographic *ac* plane. Hydrogen bonds are indicated as orange dashed lines. Symmetry codes are given in Table 2. (For interpretation of the references to colour in this figure legend, the reader is referred to the web version of this article).

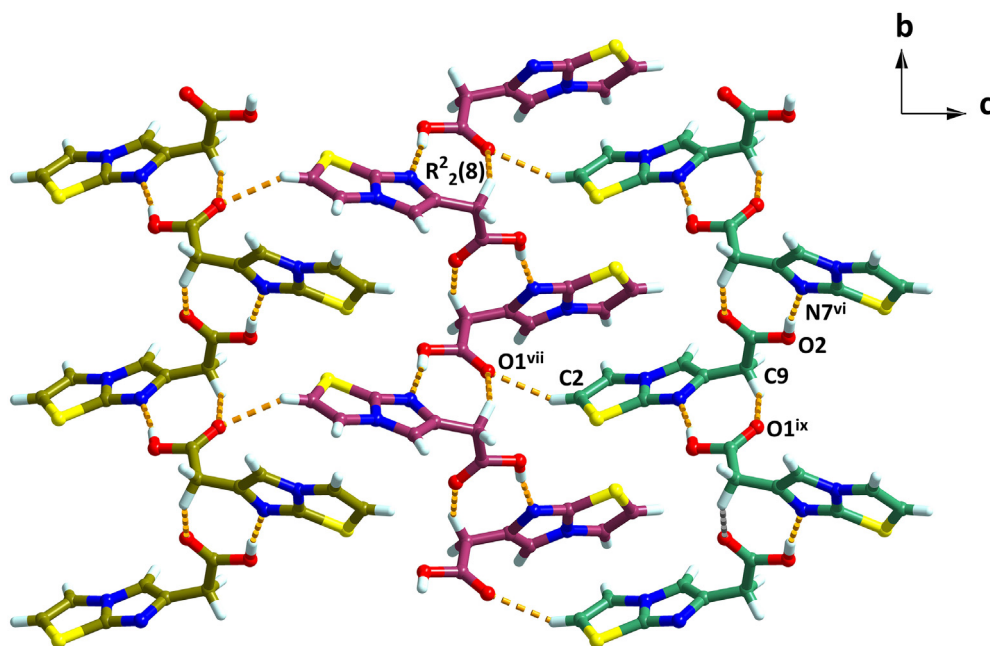


Fig. 3. A packing diagram for **2** showing selected C–H···O interactions between neighbouring zig–zag tapes (shown in dark yellow, magenta and green) in the crystallographic *bc* plane. Hydrogen bonds are indicated as orange dashed lines. Symmetry codes are given in Table 2. (For interpretation of the references to colour in this figure legend, the reader is referred to the web version of this article).

As discussed above, analysis of interactions and packing in **1** and **2** reveals presence of O–H···N hydrogen bonded zig–zag tapes, combined into a three-dimensional crystal lattice by means of C–H···O interactions. The O–H···N short contacts formed between carboxylic substituents and imidazole nitrogen atoms are visible on corresponding d_{norm} Hirshfeld surfaces as red areas (Fig. 4a), whereas on respective fingerprint plots (Fig. 4b) sharp spikes in the upper (H···N, donor) and lower (N···H, acceptor)

region can be seen. Comparable lengths of spikes illustrate similar D···A distances in both compounds. In total the H···N/N···H contacts contribute to 22.6% and 16.8% of surface areas in **1** and **2**, respectively (Fig. 5).

Weaker C–H···O type interactions (Table 2) can be seen on corresponding d_{norm} plots as pale-red areas (Fig. 4a) and contribute to two short H···O/O···H spikes in the fingerprint plots (Fig. 4b). In all, H···O/O···H contacts constitute 26.1% and 20.4% Hirshfeld

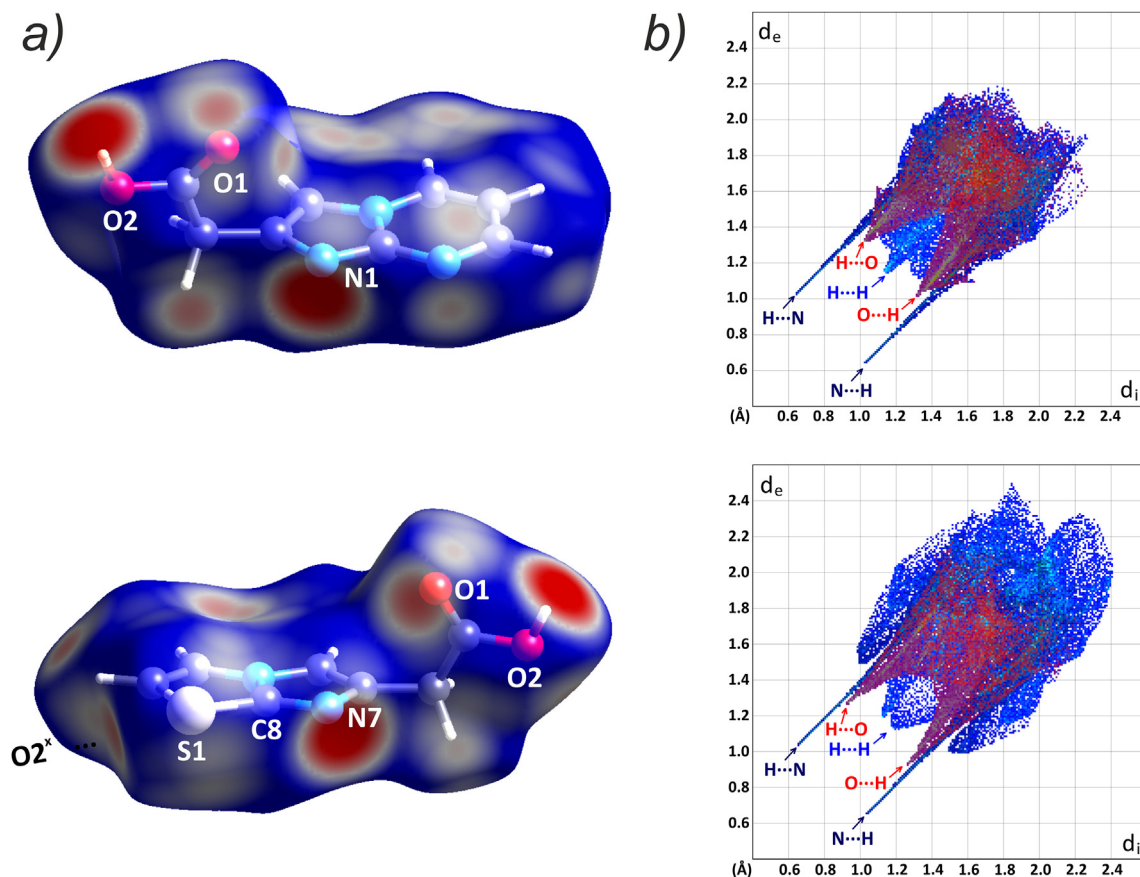


Fig. 4. (a) Hirshfeld surfaces of **1** (upper) and **2** (lower) showing views of d_{norm} (from -0.5 \AA (blue) to 0.5 \AA (red)) as well as selected atom labels; (b) 2D fingerprint plots for **1** (upper) and **2** (lower). (For interpretation of the references to colour in this figure legend, the reader is referred to the web version of this article).

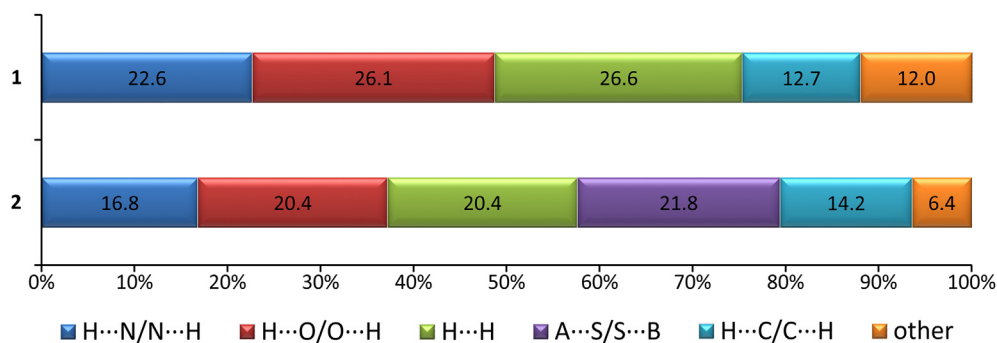


Fig. 5. Close contacts contributions to the Hirshfeld surface areas in the crystal structures of **1** and **2** divided into major interaction types (shown in percentage of total Hirshfeld surface areas).

surface areas in **1** and **2**, respectively (Fig. 5).

Remaining pale areas seen in vicinity of molecule backbones (Fig. 4a) correspond to other types of contacts, including most dominant $\text{H}\cdots\text{H}$ (26.6% and 20.4% total surface area in **1** and **2**, respectively, seen as short spikes in fingerprint plots (Fig. 4b) and $\text{H}\cdots\text{C}/\text{C}\cdots\text{H}$ (total 12.7% and 14.2% surface area in **1** and **2**, respectively). The latter can be indicative of $\text{C}-\text{H}\cdots\pi$ interactions (not discussed here).

A distinct feature of **2** is the presence of a sulfur atom, contacts of which are visible on the d_{norm} plot (Fig. 4a). In that case, 10.3% of the total Hirshfeld surface of **2** is composed by $\text{H}\cdots\text{S}/\text{S}\cdots\text{H}$ contacts (seen as pale diffuse area in vicinity of sulfur). Whereas other

contact types involving the S atom individually contribute to less than 5% of the surface, in total they constitute as much as 21.8% of Hirshfeld surface in the crystal structure of **2**.

Interestingly, the d_{norm} plot shows a distinct pale-red spot corresponding to a $\text{S}\cdots\text{O}$ contact ($2.999(2) \text{ \AA}$). As studied previously, intermolecular $\text{S}\cdots\text{O}$ contacts are typically arranged in a defined pattern [31] where nucleophilic atoms are likely to form a contact along the extension of the primary $\text{C}-\text{S}$ bond. In case of crystal structure of **2**, a corresponding $\text{C8}-\text{S1}\cdots\text{O2}$ angle equals $161.8(1)^\circ$, being in acceptable agreement with typically observed geometry.

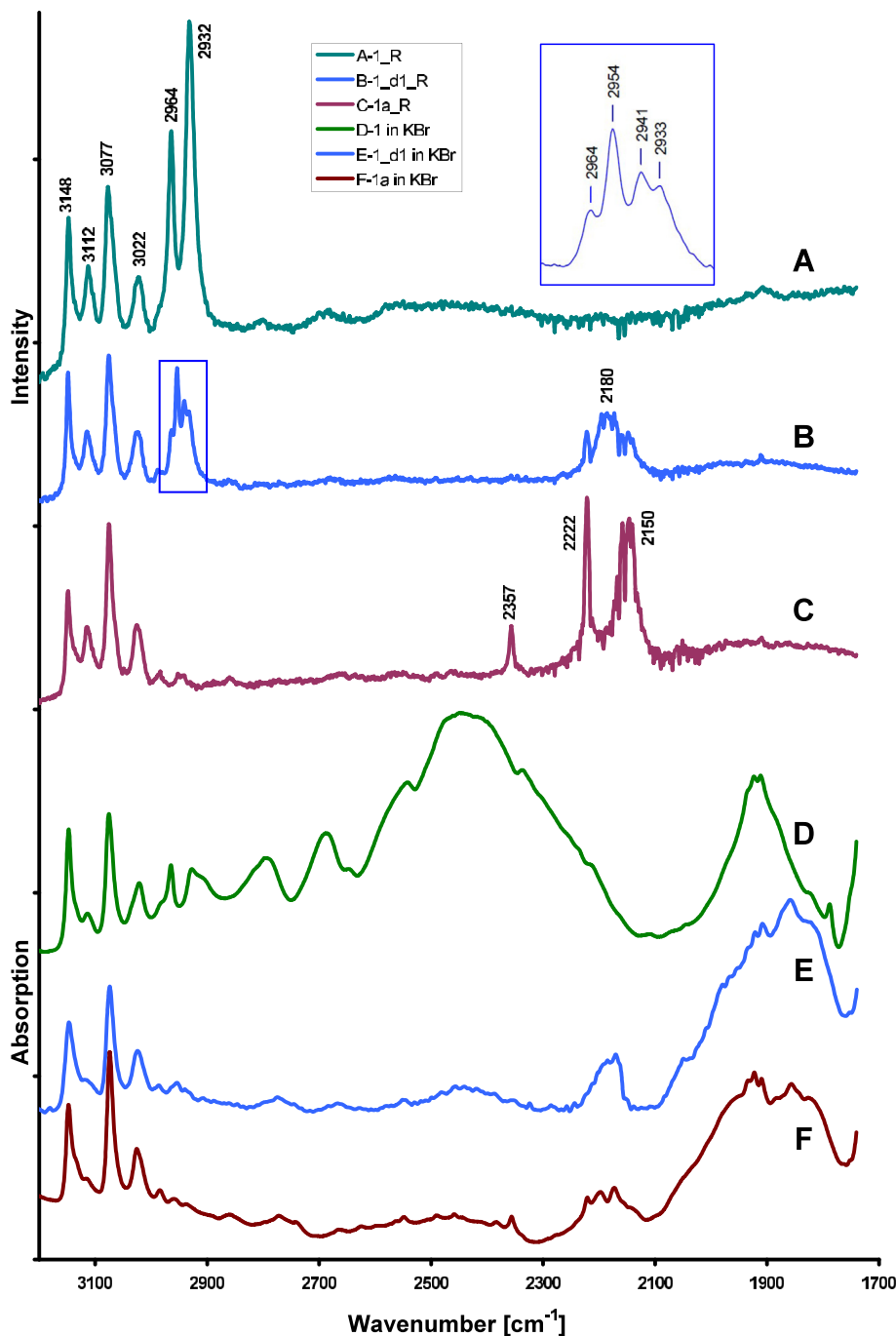


Fig. 6. Raman (A, B, C) and IR (D, E, F) spectra of **1** with groups: OH and CH₂ (A, D), OD, CHD and CD₂ (B, E), OD and CD₂ (C, F).

3.4. Spectral analysis of **1** and **2**

The vibrational spectra of *HIPM-2-ac* (**1**) and *HITZ-6-ac* (**2**) were interpreted with the aid of DFT calculations and PED analysis of computed normal vibrations. The calculations were carried out for single molecules (Fig. S6) and did not consider the O–H···N hydrogen bonding present in the crystalline state. As the normal modes with contributions of OH group vibrations cannot be correlated easily with observed bands, the spectra of deuterated isotopologues **1a** and **2a** were also collected and compared with those of parent compounds (Fig. S7).

Visual comparison of mentioned spectra indicates that

deuteration causes much more spectral changes than expected for one stretching and two bending modes of OH group. This problem can be explained by considering the Raman of 1700–3200 cm⁻¹ region presented for **1** together with related IR spectra in Fig. 6. Comparison of spectra A and C in the 2900–3000 cm⁻¹ region clearly shows that two bands at 2964 and 2932 cm⁻¹, corresponding to asymmetric and symmetric CH₂ stretching vibrations, disappeared upon typical three-fold sample **1** recrystallization from D₂O solution, indicating that methylene group was also deuterated. Our attempt to prepare (by single recrystallization) the isotopologue with O–H group exclusively deuterated was unsuccessful, but enabled monitoring an interesting feature seen in

spectrum B. The intensity lowering of two bands at 2964 and 2932 cm^{-1} is accompanied by raising of two new bands at 2954 and 2941 cm^{-1} (see Fig. 6 inset). Such changes correspond to partial deuteration of CH_2 groups. New bands result from stretching vibrations of single C–H bond in the monodeuterated CHD group. These bands are located between $\nu_a(\text{CH}_2)$ and $\nu_s(\text{CH}_2)$ which has been confirmed by DFT calculations where $\nu(\text{C–H10A}) = 2965$ and $\nu(\text{C–H10B}) = 2964 \text{ cm}^{-1}$.

Similar calculations for parent compound **1** gave $\nu_a(\text{CH}_2) = 2983$ and $\nu_s(\text{CH}_2) = 2945 \text{ cm}^{-1}$ (mentioned calculated wavenumbers are 0.96 scaled). Wavenumber comparison of observed (Fig. 6 inset) and calculated $\nu(\text{C–H})$ vibrations for CHD group shows that former are more separated (13 cm^{-1}) than latter (1.0 cm^{-1}). Larger separation may be explained by different interaction of methylene hydrogen atoms with neighbor molecules. The X-ray measurements show that only H10A atom of **1** (see Fig. 1a for atom numbering and Table 2) is involved in C–H \cdots O contact. Thus, assuming typical “red shift” of $\nu(\text{C–H})$ energy upon hydrogen bond formation [32], the band at 2941 cm^{-1} can be attributed to the $\nu(\text{C–H10A})$ stretching vibration, whereas band at 2954 cm^{-1} to $\nu(\text{C–H10B})$ mode. The $\nu(\text{C–D})$ counterparts of discussed CHD group vibrations are observed as broader band centered at 2180 cm^{-1} . Besides this band, two other bands at 2222 and 2150 cm^{-1} reveal that fully deuterated CD_2 groups are also present (compare with spectrum C in Fig. 6). Spectrum C also confirms that after three-fold recrystallization from D_2O solution, the methylene group deuteration is almost complete. Additional band at 2357 cm^{-1} , which Raman intensity grows along the deuteration progress, probably results from the overtone of 1322 cm^{-1} strong vibration. The deuteration of methylene group is also confirmed by respective IR measurements (spectra E and F in Fig. 6).

These observations are strongly supported by ^1H NMR studies in solution. To gain insight into H/D exchange in CH_2 groups of **1**, the spectra of its D_2O solution were recorded as a function of time (Fig. 7, for full spectra see Figs. S8 and S9). It would be evident, that the CH_2 resonance disappears almost completely within ca. three days and only small intensity signal attributed to CHD group is present in the spectrum. Similar result confirming almost complete deuteration of CH_2 groups in D_2O solution was obtained for triply deuterated **1a**. Interestingly, analogous experiment performed for **2** revealed much less effective replacement of its methylene hydrogen atoms by deuterium. Therefore, we attempted to avoid H/D exchange in the CH_2 groups by using CD_3OD for recrystallization of **2**. A complete suppression of H/D exchange in CH_2 groups of **2a** is confirmed by its ^1H NMR spectrum (Fig. 7g) and clearly reflected in Raman spectrum, where bands at 2965 and 2920 cm^{-1} were fully preserved.

The observed positions of vibrational bands and their assignments are summarized in Table 3 for **1**, **1a** and Table 4 for **2**, **2a**, respectively. The wavenumber correlation between corresponding IR and Raman bands is very good, as has been presented graphically in Fig. S10 and as it results from MAE values not exceeding the 2.5 cm^{-1} . Since the main goal of this work was the characterization of the observed spectra, the normal modes of extremely low IR intensities and Raman activities were excluded and are not listed in respective Tables. Special attention was paid on vibrations of hydroxyl and methylene groups involved in hydrogen bonds, which may substantially change their wavenumbers and cause larger discrepancies with respective calculated values. Fortunately, both groups in **1** are sensitive to deuteration and recorded H/D substitution spectral effects were used for respective band detection. Comparison of normal vibrations collected for **1** and **1a** in Table 3 shows that thirteen modes are changed upon deuteration in the 1800–400 cm^{-1} region. The contributions of deformation modes of OH and CH_2 groups have been found in ten of these modes, which

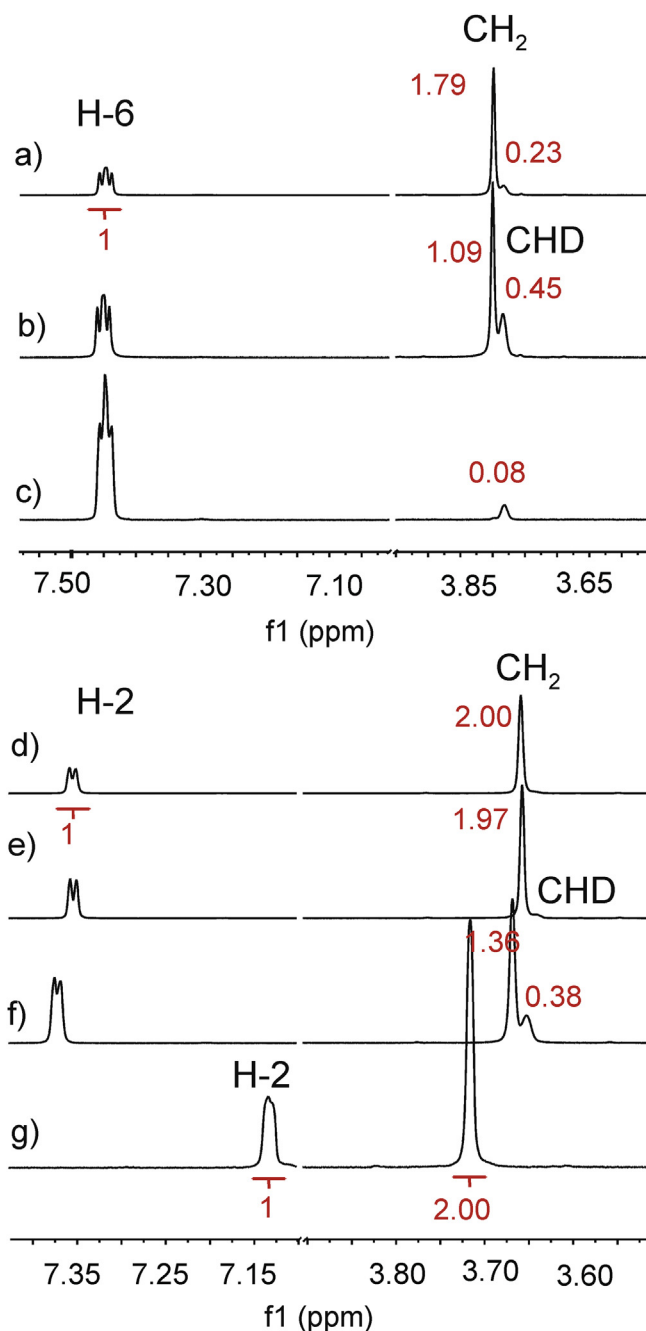


Fig. 7. The H-6/H-2 and CH_2 resonances in the ^1H NMR spectra of D_2O solutions of **1** (a–c) and **2** (d–f) measured for freshly prepared samples, after one day and after three days, respectively, and spectrum of CD_3OD solution of **2a** (g). Integrals are given in red. For the sake of clarity signals of solvents are removed. (Complete spectra and their assignments are given in Figs. S1–S4). (For interpretation of the references to colour in this figure legend, the reader is referred to the web version of this article).

are more than expected (two for OH and four for CH_2 in discussed wavenumber region). This is a result of coupling of $\delta(\text{OH})$ and $\gamma(\text{OH})$ with other internal modes as well as of additional contribution of $\rho_r(\text{CH}_2)$ in 511 cm^{-1} normal vibration. The remaining deformation modes of methylene group are coupled in different extent. The scissoring and twisting internal modes show 75 and 88% PED contributions in 1475 and 1234 cm^{-1} normal vibrations, whereas the highest contributions of wagging and rocking modes are 32 and 36% in 1429 and 993 cm^{-1} vibrations, respectively. All these vibrations were attributed to observed bands sensitive to

Table 3

Selection of observed and calculated IR and Raman bands [cm^{-1}], attributed to vibrations of parent HIPM-2-ac (**1**) and its OD/CD₂ isotopologue **1a** with their general and PED based assignments. (Atoms numbering scheme is consistent with that provided in Fig. 1a).

Observed ^a		Calculated		General assignment ^{b,c}	Selected PED terms ^c (mostly $\geq 10\%$)	
1	1a	1	1a			
IR	Raman	IR	Raman	[IR int, R activ]	[IR int, R activ]	
2965w	2964m	2983 ^d		$\nu_a(\text{CH}_2)$	$\nu(\text{C}_{10}-\text{H}_{10\text{B}})-51 + \nu(\text{C}_{10}-\text{H}_{10\text{A}})-49$	
2928w	2932m	[1,29] 2945 ^d [8,90]		$\nu_s(\text{CH}_2)$	$\nu(\text{C}_{10}-\text{H}_{10\text{A}})-50 + \nu(\text{C}_{10}-\text{H}_{10\text{B}})-49$	
	2212w	2222m		$\nu_a(\text{CD}_2)$	$\nu(\text{C}_{10}-\text{D}_{10\text{B}})-51 + \nu(\text{C}_{10}-\text{D}_{10\text{A}})-49$	
	2165w	2150m		2205 ^d [1,25] 2145 ^d [4,80]	$\nu(\text{C}_{10}-\text{D}_{10\text{A}})-51 + \nu(\text{C}_{10}-\text{D}_{10\text{B}})-48$	
1705s	1694w	1705s	1687w	1717 [210,3]	$\nu(\text{C}=\text{O})$	$\nu(\text{O}_1-\text{C}_{11})-86/91 + \nu(\text{C}_{10}-\text{C}_{11})-10/11$
1618s	1621m	1618s	1621m	1649 [44,20]	$\nu(\text{C}=\text{C})_{\text{pm}} + \nu(\text{N}-\text{C})_{\text{pm}}$	$\nu(\text{C}_6-\text{C}_5)-31 + \nu(\text{N}_4-\text{C}_5)-9 + \nu(\text{N}_8-\text{C}_7)-7 + \nu(\text{N}_8-\text{C}_7)-7$
1563m	1561s	1560w	1559s	1571 [49,151]	$\nu(\text{C}=\text{C})_{\text{im}} + \nu(\text{C}-\text{C})$	$\nu(\text{C}_2-\text{C}_3)-31 + \nu(\text{C}_2-\text{C}_{10})-27$
1515s	1521m	1520sh	1521s	1534 [17,37]	$\nu(\text{N}=\text{C})_{\text{im}} + \nu(\text{N}-\text{C})_{\text{pm}}$	$\nu(\text{N}_1-\text{C}_7)-24 + \nu(\text{N}_8-\text{C}_9)-17$
1454m	n.o.			1475 [47,28]	$\delta(\text{CH}_2)$	$\delta(\text{H}_{10\text{B}}-\text{C}_{10}-\text{H}_{10\text{A}})-75$
1430m	1430m	1428m	1430m	1463 [13,23]	$\nu(\text{N}-\text{C})$	$\nu(\text{N}_8-\text{C}_7)-26/29 + \nu(\text{N}_4-\text{C}_5)-12$
1404m	1406w			1429 [89,23]	$\nu(\text{C}-\text{C}) + \rho_w(\text{CH}_2)$	$\nu(\text{C}_{10}-\text{C}_{11})-15 + \delta(\text{C}_{11}-\text{C}_{10}-\text{H}_{10\text{B}})-11 + \delta(\text{C}_{11}-\text{C}_{10}-\text{H}_{10\text{A}})-11 + \nu(\text{C}_2-\text{C}_{10})-10$
1343m	1344m	1347s	1343s	1378 [5,9]	$\nu(\text{C}-\text{N})_{\text{im}} - \delta(\text{C}-\text{H})_{\text{pm}}$	$\nu(\text{N}_4-\text{C}_3)-14/7 + \delta(\text{C}_8-\text{C}_5-\text{H}_{15})-9/7$
		1347s	1343m	1348 [50,28]	$\nu(\text{N}-\text{C})_{\text{im}}$	$\nu(\text{N}_1-\text{C}_2)-19 + \nu(\text{N}_4-\text{C}_3)-10 + \nu(\text{C}_3-\text{C}_2)-10$
1319s	n.o.			1333 [3,12]	$\nu(\text{N}-\text{C})_{\text{im}} + \delta(\text{OH})$	$\nu(\text{N}_1-\text{C}_2)-18 + \delta(\text{C}_{11}-\text{O}_2-\text{H}_2)-13 + \nu(\text{O}_2-\text{C}_{11})-12$
		1322s	1324m	1298 [76,2]	$\nu(\text{C}-\text{O}) + \nu(\text{C}-\text{C})$	$\nu(\text{O}_2-\text{C}_{11})-27 + \nu(\text{C}_{11}-\text{C}_{10})-25$
1218s	n.o.			1273 [26,8]	$\delta(\text{OH})$	$\delta(\text{C}_{11}-\text{O}_2-\text{H}_2)-21$
1186s	1192m			1234 [1,8]	$\rho_t(\text{CH}_2)$	$\delta(\text{C}_{11}-\text{C}_{10}-\text{H}_{10\text{B}})-22 + \delta(\text{C}_2-\text{C}_{10}-\text{H}_{10\text{B}})-22 + \delta(\text{C}_{11}-\text{C}_{10}-\text{H}_{10\text{A}})-22 + \delta(\text{C}_2-\text{C}_{10}-\text{H}_{10\text{A}})-22$
1241sh	1240s	1226m	1231s	1227 [4,30]	$\delta(\text{CH})$	$\delta(\text{H}_3-\text{C}_3-\text{N}_4)-26 + \delta(\text{C}_2-\text{C}_3-\text{H}_3)-22$
1045m	1050m			1087 [439,4]	$\nu(\text{C}-\text{O}) + \delta(\text{OH})$	$\nu(\text{O}_2-\text{C}_{11})-54 + \delta(\text{C}_{11}-\text{O}_2-\text{H}_2)-42$
1020m	n.o.			1041 [4,21]	$\nu(\text{C}-\text{C})_{\text{pm}}$	$\nu(\text{C}_7-\text{C}_6)-28$
		1092m	1096w	1084 [28,9]	$\delta(\text{CD}_2)$	$\delta(\text{H}_{10\text{B}}-\text{C}_{10}-\text{H}_{10\text{A}})-68$
		1067m	1068w	1067 [22,19]	$\nu(\text{N}-\text{C})_{\text{im}} + \nu(\text{C}-\text{O}) + \rho_w(\text{CD}_2)$	$\nu(\text{N}_1-\text{C}_2)-16 + \nu(\text{C}_{11}-\text{O}_2)-12 + \delta(\text{C}_{11}-\text{C}_{10}-\text{H}_{10\text{A}})-8 + \delta(\text{C}_{11}-\text{C}_{10}-\text{H}_{10\text{B}})-8$
1002m	1004w			1002 [29,4]	$\nu(\text{C}-\text{C})$	$\nu(\text{C}_2-\text{C}_{10})-11$
958w	953m			993 [15,2]	$\pi(\text{C}=\text{O}) + \rho_r(\text{CH}_2)$	$\pi(\text{O}_1-\text{C}_{11}, \text{C}_{10}, \text{O}_2)-15 + \delta(\text{C}_2-\text{C}_{10}-\text{H}_{10\text{A}})-13 + \delta(\text{C}_2-\text{C}_{10}-\text{H}_{10\text{B}})-13$
		970m	973m	967 [57,1]	$\delta(\text{OD}) + \nu(\text{C}-\text{O})$	$\delta(\text{C}_{11}-\text{O}_2-\text{D}_2)-26 + \nu(\text{C}_{11}-\text{O}_2)-10$
		954m	962w	961 [74,20]	$\nu(\text{C}-\text{O}) + \delta(\text{OD})$	$\nu(\text{C}_{11}-\text{O}_2)-31 + \delta(\text{C}_{11}-\text{O}_2-\text{D}_2)-24$
		935m	934m	944 [3,3]	$\rho_t(\text{CD}_2) + \pi(\text{C}=\text{O})$	$\delta(\text{C}_{11}-\text{C}_{10}-\text{D}_{10\text{B}})-23 + \delta(\text{C}_{11}-\text{C}_{10}-\text{D}_{10\text{A}})-23 + \pi(\text{O}_1-\text{C}_{11}, \text{C}_{10}, \text{O}_2)-20$
		828w	n.o.	903 [19,3]	$\rho_t(\text{CD}_2)$	$\delta(\text{C}_2-\text{C}_{10}-\text{H}_{10\text{A}})-18 + \delta(\text{C}_2-\text{C}_{10}-\text{H}_{10\text{B}})-18 + \pi(\text{H}_3-\text{C}_3, \text{C}_2, \text{N}_4)-17$
895m	895m			899 [1,24]	$\nu(\text{C}-\text{C}) + \nu(\text{C}-\text{O})$	$\nu(\text{C}_{10}-\text{C}_{11})-43 + \nu(\text{O}_2-\text{C}_{11})-12$
794s	795w	794m	804m	806 [1,36]	$\nu(\text{N}-\text{C})$	$\nu(\text{N}_4-\text{C}_9)-22/16$
723s	723w			676 [43,2]	$\delta(\text{im}) + \pi(\text{C}=\text{O}) + \gamma(\text{OH}) + \pi(\text{CC})$	$\gamma(\text{N}_1-\text{C}_2-\text{C}_3-\text{N}_4)-21/23 + \pi(\text{O}_1-\text{C}_{11}, \text{C}_{10}, \text{O}_2)-15/9 + \gamma(\text{H}_2-\text{O}_2-\text{C}_{11}-\text{O}_1)-10/0 + \pi(\text{C}_{10}-\text{C}_2, \text{C}_3, \text{N}_1)-10/8$
		714s	714w	647 [9,3]	$\delta(\text{im}) + \pi(\text{C}=\text{O}) + \pi(\text{CC})$	$\gamma(\text{N}_1-\text{C}_2-\text{C}_3-\text{N}_4)-21 + \pi(\text{O}_1-\text{C}_{11}, \text{C}_{10}, \text{O}_2)-15 + \pi(\text{C}_{10}-\text{C}_2, \text{C}_3, \text{N}_1)-10$
675s	675m			642 [124,7]	$\gamma(\text{OH}) + \pi(\text{C}=\text{O})$	$(\text{H}_2-\text{O}_2-\text{C}_{11}-\text{O}_1)-90 + \pi(\text{O}_1-\text{C}_{11}, \text{C}_{10}, \text{O}_2)-8$
638m	640m	646m	647m	641 [1,17]	$\nu(\text{C}-\text{N})_{\text{pm}} + \delta(\text{CNC})$	$\nu(\text{N}_8-\text{C}_9)-7 + \nu(\text{N}_4-\text{C}_5)-6 + \delta(\text{C}_3-\text{N}_4-\text{C}_9)-6 + \delta(\text{C}_6-\text{C}_7-\text{N}_8)-6$
		520w	525w	530 [48,1]	$\gamma(\text{OD}) + \pi(\text{C}=\text{O})$	$\gamma(\text{H}_2-\text{O}_2-\text{C}_{11}-\text{O}_1)-65 + \pi(\text{O}_1-\text{C}_{11}, \text{C}_{10}, \text{O}_2)-35$
n.o.	493m			511 [29,10]	$\pi(\text{C}=\text{O}) + \rho_t(\text{CH}_2)$	$\pi(\text{O}_1-\text{C}_{11}, \text{C}_{10}, \text{O}_2)-65 + \delta(\text{C}_{11}-\text{C}_{10}-\text{H}_{10\text{A}})-9 + \delta(\text{C}_{11}-\text{C}_{10}-\text{H}_{10\text{B}})-9$
		460w	461w	523 [53,29]	$\delta(\text{OCO}) + \delta(\text{OD})$	$\delta(\text{O}_2-\text{C}_{11}-\text{O}_1)-24 + \delta(\text{C}_{11}-\text{O}_2-\text{D}_2)-17$
446w	450m	443w	449m	450 [1,5]	$\delta(\text{pm}) + \pi(\text{CH}_{14})$	$\gamma(\text{C}_7-\text{C}_6-\text{C}_5-\text{N}_4)-26/24 + \pi(\text{H}_6-\text{C}_6, \text{C}_5, \text{C}_7)-19/18 + \gamma(\text{C}_5-\text{N}_4-\text{C}_3-\text{C}_2)-11/11 + \gamma(\text{C}_9-\text{N}_8-\text{C}_7-\text{C}_6)-9/8$
		443w	449m	408 [36,4]	$\gamma(\text{OD}) + \pi(\text{C}=\text{O})$	$\gamma(\text{D}_2-\text{O}_2-\text{C}_{11}-\text{O}_1)-31 + \pi(\text{O}_1-\text{C}_{11}, \text{C}_{10}, \text{O}_2)-27$

^a s – strong, m – medium, w – weak, sh – shoulder, n.o. – not observed.

^b ν_a – antisymmetric stretching, ν_s – symmetric stretching, δ – bending in-plane, ρ_t – twisting, ρ_w – wagging, ρ_r – rocking, π – bending out-of-plane, γ – torsion, im/pm – imidazole/pyrimidine ring.

^c – the slash separates the PED values for parent and deuterated compound.

^d – calculated wavenumbers were scaled by 0.96.

deuteration. For example, the CH₂ twisting mode, calculated at 1234 cm^{-1} , was not attributed to nearest Raman band at 1240 cm^{-1} , but to band at 1192 cm^{-1} because in the 1250–1150 cm^{-1} region, this is the only band which disappears upon deuteration. The

deuteration also confirmed the localization of bands related to vibrations only partially affected by H/D replacement. One of such vibrations is the $\nu(\text{C}-\text{C}) + \nu(\text{C}-\text{O})$ mode calculated at 899 cm^{-1} which has no counterpart in the theoretical spectra of deuterated

Table 4
Selection of observed and calculated IR and Raman bands [cm^{-1}] attributed to vibrations of parent *HITZ-6-ac* (**2**) and its OD isotopologue **2a** with their general and PED based assignments. (Atoms numbering scheme is consistent with that provided in Fig. 1b).

Observed ^a				Calculated – 0.96 scaled		General assignment ^{b,c}	Selected PED terms ^c (mostly $\geq 10\%$)
H ₂ O		D ₂ O		H ₂ O	D ₂ O		
IR	Raman	IR	Raman	[IR int, R activ]	[IR int, R activ]		
n.o.	2966m	2965w	2965m	2998 ^d [2,28]	2998 ^d [2,28]	$\nu_a(\text{CH}_2)$	$\nu(\text{C}_9\text{--H}_{9A})\text{--}50 + \nu(\text{C}_9\text{--H}_{9B})\text{--}50$
2915w	2923m	2918w	2920m	2940 ^d [12,80]	2940 ^d [12,80]	$\nu_s(\text{CH}_2)$	$\nu(\text{C}_9\text{--H}_{9B})\text{--}50 + \nu(\text{C}_9\text{--H}_{9A})\text{--}49$
1704m	1699w	1698s	1692w	1717 [205,4]	1708 [190,4]	$\nu(\text{C}=\text{O})$	$\nu(\text{O}_1\text{--C}_{10})\text{--}86 + \nu(\text{C}_9\text{--C}_{10})\text{--}10$
1567m	1569s	1567m	1568s	1607 [48,101]	1607 [48,101]	$\nu(\text{C}=\text{C})_{\text{th}}$	$\nu(\text{C}_8\text{--C}_3)\text{--}44$
1543m	1547w	1544m	1546w	1586 [1,7]	1586 [1,7]	$\nu(\text{C}=\text{C})_{\text{im}}$	$\nu(\text{C}_6\text{--C}_5)\text{--}33 + \nu(\text{C}_6\text{--C}_9)\text{--}22$
1448m	1458w	1454s	1461w	1485 [60,12]	1485 [60,12]	$\nu(\text{C}=\text{N})_{\text{im}} + \delta(\text{CH}_2)$	$\nu(\text{N}_7\text{--C}_2)\text{--}33 + \delta(\text{H}_{9B}\text{--C}_9\text{--H}_{9A})\text{--}25$ $\delta(\text{H}_{9B}\text{--C}_9\text{--H}_{9B})\text{--}52 - \nu(\text{N}_7\text{--C}_8)\text{--}17$
1331s	1339w	1325s	1314m	1314 [5,15]	1281 [7,19]	$\delta(\text{OH}) + \nu(\text{C--O})$	$\delta(\text{C}_{10}\text{--O}_2\text{--H}_{20})\text{--}25 + \nu(\text{O}_2\text{--C}_{10})\text{--}14$
1214s	n.o.	1232m	n.o.	1231 [22,4]	1181	$\nu(\text{C--N})_{\text{im}} + \nu(\text{C--O})$	$\nu(\text{N}_7\text{--C}_6)\text{--}21 + \nu(\text{O}_2\text{--C}_{10})\text{--}11$
		1184m	1189m		[160,15]	$\nu(\text{C--O}) + \delta(\text{OH})$	$\nu(\text{N}_7\text{--C}_6)\text{--}21 + \delta(\text{C}_{10}\text{--O}_2\text{--H}_{20})\text{--}14$ $\nu(\text{O}_2\text{--C}_{10})\text{--}21 + \nu(\text{N}_7\text{--C}_8)\text{--}11$
1178s	1181m			1088 [328,8]		$\nu(\text{C--O}) + \delta(\text{OH})$	$\nu(\text{O}_2\text{--C}_{10})\text{--}40 + \delta(\text{C}_{10}\text{--O}_2\text{--H}_{20})\text{--}32$
1000s	1001m	999m	999m	986 [24,15]	989 [7,23]	$\nu(\text{C--N})_{\text{im}}$	$\nu(\text{N}_7\text{--C}_6)\text{--}23/21$
		1077m	1080w		965 [151,7]	$\nu(\text{C--O}) + \delta(\text{OD})$	$\nu(\text{O}_2\text{--C}_{10})\text{--}45 + \delta(\text{C}_{10}\text{--O}_2\text{--D}_{20})\text{--}42$
897m	902m			905 [6,22]		$\nu(\text{C--C}) + \nu(\text{C--O})$	$\nu(\text{C}_9\text{--C}_{10})\text{--}41 + \nu(\text{O}_2\text{--C}_{10})\text{--}13$
		858m	n.o.		876 [5,12]	$\nu(\text{C--C}) + \delta(\text{OD})$	$\nu(\text{C}_9\text{--C}_{10})\text{--}25 + \delta(\text{C}_{10}\text{--O}_2\text{--D}_{20})\text{--}17$
862m	864w	869m	877m	895 [2,8]	895 [2,8]	$\pi(\text{CH}_{10}) - \pi(\text{CH}_{12})$	$\pi(\text{H}_3\text{--C}_3, \text{C}_5, \text{N}_4)\text{--}68 + \pi(\text{H}_2\text{--C}_8, \text{C}_3, \text{S}_1)\text{--}28$
768s	768vw	766m	765w	810 [49,4]	810 [49,4]	$\pi(\text{CH})_{\text{im}}$	$\pi(\text{H}_5\text{--C}_5, \text{C}_6, \text{N}_4)\text{--}95$
746s	746m	743m	744m	739 [34,1]	739 [34,1]	$\pi(\text{CH}_{12}) + \pi(\text{CH}_{10}) + \tau_1(\text{im})$	$\pi(\text{H}_2\text{--C}_8, \text{C}_3, \text{S}_1)\text{--}37 + \pi(\text{H}_3\text{--C}_3, \text{C}_8, \text{N}_4)\text{--}28 + \pi(\text{N}_4\text{--C}_2, \text{N}_7, \text{S}_1)\text{--}17$
725s	720w	719s	719w	706 [3,20]	705 [4,22]	$\nu(\text{S--C})$	$\nu(\text{S}_1\text{--C}_8)\text{--}40/42$
666s	670w	665s	666w	673 [24,1]	673 [41,2]	$\pi(\text{CH}_{12}) + \pi(\text{CH}_{10}) - \tau_1(\text{im})$	$\pi(\text{H}_2\text{--C}_8, \text{C}_3, \text{S}_1)\text{--}39/42 + \pi(\text{N}_4\text{--C}_2, \text{N}_7, \text{S}_1)\text{--}27/28 + \pi(\text{H}_3\text{--C}_3, \text{C}_8, \text{N}_4)\text{--}13/14 + \gamma(\text{C}_2\text{--N}_7\text{--C}_6\text{--C}_5)\text{--}12/11$
692m	695w			640 [106,5]		$\gamma(\text{OH}) + \pi(\text{C}=\text{O})$	$\gamma(\text{H}_{20}\text{--O}_2\text{--C}_{10}\text{--O}_1)\text{--}84 + \pi(\text{O}_1\text{--C}_{10}, \text{C}_9, \text{O}_2)\text{--}9$
597w	599m			626 [26,6]	611 [9,2]	$\nu(\text{S--C}) + \delta(\text{OCO})$	$\nu(\text{S}_1\text{--C}_8)\text{--}17 + \delta(\text{O}_1\text{--C}_{10}\text{--O}_2)\text{--}12$
		592w	594m			$\nu(\text{S--C})$	$\nu(\text{S}_1\text{--C}_8)\text{--}21$
568w	568m			574 [35,17]		$\delta(\text{OCO})$	$\delta(\text{O}_1\text{--C}_{10}\text{--O}_2)\text{--}15$
		553m	557m		547 [30,19]	$\delta(\text{OCO}) + \delta(\text{OD})$	$\delta(\text{O}_1\text{--C}_{10}\text{--O}_2)\text{--}16 + \delta(\text{C}_{10}\text{--O}_2\text{--D}_{20})\text{--}14$
555s	559m	553m	557m	540 [15,20]	538 [37,19]	$\nu(\text{S--C})$	$\nu(\text{S}_1\text{--C}_2)\text{--}18 + \delta(\text{C}_8\text{--S}_1\text{--C}_2)\text{--}12/\nu(\text{S}_1\text{--C}_2)\text{--}14$
448m	449w	447m	448w	458 [5,3]	455 [9,4]	$\nu(\text{S--C}) + \delta(\text{NCS})$	$\nu(\text{S}_1\text{--C}_2)\text{--}19 + \delta(\text{N}_7\text{--C}_2\text{--S}_1)\text{--}11/10$

^a s – strong, m – medium, w – weak, sh – shoulder, n.o. – not observed.

^b ν_a – antisymmetric stretching, ν_s – symmetric stretching, δ – bending in-plane, ρ_t – twisting, ρ_w – wagging, ρ_r – rocking, π – bending out-of-plane, γ – torsion, im/th – imidazole/thiazole ring.

^c – The slash separates the assignment for parent and deuterated compound.

^d – calculated wavenumbers were scaled by 0.96.

compound **1a**. Similar behavior shows the 895 cm^{-1} IR and Raman band not observed in the spectrum of deuterated compound.

As expected for **2**, almost exclusive deuteration of carboxylic OH groups caused less spectral changes than in case of **1**. Comparison of IR spectra of **2** and **2a** shows intensity decrease for group of bands between 1335 and 1295 cm^{-1} as well as bands at 1214 , 1178 , 897 , 692 and 568 cm^{-1} whereas new bands are observed at 1232 , 1077 and 858 cm^{-1} in spectrum of **2a**. As results from theoretical calculations, first three changes are caused by $\delta(\text{OH})$ bending vibration, which contributes in three normal modes at 1314 , 1231 and 1088 cm^{-1} together with stretching vibrations of C–N and C–O bonds. The band at 897 cm^{-1} shifts to 858 cm^{-1} as a result of additional coupling with $\delta(\text{OD})$. Vanishing of 692 cm^{-1} band is due to torsion vibration of hydroxyl hydrogen, calculated at 640 cm^{-1} . The deuteration effect of the lowest wavenumber band (568 cm^{-1}) is a shift of $\delta(\text{OCO})$ vibration, predicted at 574 cm^{-1} for **2** and at 547 cm^{-1} (coupled with $\delta(\text{OD})$) for **2a**. For some of the recently presented modes, the difference between calculated and observed wavenumbers is relatively large, but this is the advantage of performing deuteration. Otherwise, these calculated vibrations would

be attributed to the nearest positioned bands, without knowing that this is erroneous.

In general, most of the measured bands were well correlated with calculated normal modes which characterization in PED terms also describes the vibrational character of correlated bands. Exception was made for bands observed below 400 cm^{-1} . The bands observed there are much more intense than theoretically predicted normal vibrations. This suggests that the vibrations of hydrogen bonds and lattice modes contribute in this region. This assumption is also supported by very high intensity of Raman bands at 138 , 104 and 98 cm^{-1} (compound **1**) and at 119 and 80 cm^{-1} (compound **2**), which is typical for molecular crystals.

4. Conclusions

Imidazo[1,2-*a*]pyrimidin-2-yl-acetic acid (*HIPM-2-ac*, **1**) and its analog containing imidazo[2,1-*b*]thiazole ring (*HITZ-6-ac*, **2**) were synthesized and structurally characterized by single-crystal X-ray diffraction. Both compounds crystallize as electrically neutral molecules in non-centrosymmetric *Pca*₂₁ and *P2*₁*2*₁*2*₁ space groups

of the orthorhombic crystal system, respectively. The crystals of *HIPM-2-ac* and *HITZ-6-ac* comprise similar zig-zag tapes of molecules connected by O–H···N and C–H···O interactions, joined into 3D structures by C–H···O-type contacts.

Inspection of corresponding Hirshfeld surfaces provided an additional, qualitative and quantitative insight into similarities and differences between interactions in the crystals of **1** and **2**. A distinct feature of crystal **2** is the presence of close contacts involving the S atom, which constitute as much as 21.8% of the total Hirshfeld surface area. Among them, the most prominent are H···S/S···H contacts accounting for 10.3% of the Hirshfeld surface. A noticeable is also the presence of S···O contact (2.999(2) Å) along the extension of the primary C–S bond.

The vibrational IR and Raman spectra of *HIPM-2-ac* (**1**) and *HITZ-6-ac* (**2**) were recorded and interpreted in details with the aid of DFT calculations and PED analysis of computed normal vibrations. The spectra of deuterated isotopologues **1a** and **2a** were also collected and compared with those of parent compounds. Special attention was paid on hydroxyl and methylene groups involved in hydrogen bonds, which may substantially change their wavenumbers and cause larger discrepancies with respective calculated values. Fortunately, recrystallization of **1** from D₂O solution resulted in deuteration of carboxylic OH groups and almost complete deuteration of CH₂ groups, which was employed for respective band assignments. On the other hand, deuteration of CH₂ groups of **2** under similar conditions was less effective. Indeed, complete suppression of H/D exchange in methylene groups was achieved in **2a** obtained by recrystallization from CD₃OD. This is clearly reflected in the vibrational spectra of **1**, **1a** and **2**, **2a**, respectively, and supported by ¹H NMR studies in solution.

In general, most of the vibrational bands in the IR and Raman spectra of *HIPM-2-ac* (**1**) and *HITZ-6-ac* (**2**) are well correlated with calculated normal modes. The exception are bands observed below 400 cm⁻¹ where vibrations of hydrogen bonds and lattice modes contribute.

Acknowledgments

Financial support by a statutory activity subsidy from the Polish Ministry of Science and Higher Education for the Department of Chemistry of Wrocław University of Technology is gratefully acknowledged. We also gratefully acknowledge the instrumental grant 6221/IA/119/2012 from Polish Ministry of Science and Higher Education, which supported our Integrated Laboratory of Research and Engineering of Advanced Materials where IR measurements were performed.

Appendix A. Supplementary data

Supplementary data related to this article can be found at <http://dx.doi.org/10.1016/j.molstruc.2016.03.055>.

References

- [1] A.K. Bagdi, S. Santra, K. Monir, A. Hajra, *Chem. Commun.* 51 (2015) 1555–1575.
- [2] C. Enguehard-Gueffier, A. Gueffier, *Mini Rev. Med. Chem.* 7 (2007) 888–899.
- [3] C. Hulme, Y.-S. Lee, *Mol. Divers* 12 (2008) 1–15.

- [4] (a) N. Devi, R.K. Rawal, V. Singh, *Tetrahedron* 71 (2015) 183–232; (b) G. Qian, B. Liu, Q. Tan, S. Zhang, B. Xu, *Eur. J. Org. Chem.* (2014) 4837–4843.
- [5] M.L. Fascio, M.I. Errea, N.B. D'Accorso, *Eur. J. Med. Chem.* 90 (2015) 666–683.
- [6] (a) W.R. Tully, C.R. Gardner, R.J. Gillespie, R. Westwood, *J. Med. Chem.* 34 (1991) 2060–2067; (b) W.P. Blackaby, J.R. Atack, F. Bromidge, J.L. Castro, S.C. Goodacre, D.J. Hallett, R.T. Lewis, G.R. Marshall, A. Pike, A.J. Smith, L.J. Street, D.F.D. Tattersall, K.A. Wafford, *Bioorg. Med. Chem. Lett.* 16 (2006) 1175–1179.
- [7] (a) T.H. Al-Tel, R.A. Al-Qawasmeh, *Eur. J. Med. Chem.* 45 (2010) 5848–5855; (b) T. Juspin, M. Laget, T. Terme, N. Azas, P. Vanelle, *Eur. J. Med. Chem.* 45 (2010) 840–845.
- [8] A. Marwaha, J. White, F. El Mazouni, S.A. Creason, S. Kokkonda, F.S. Buckner, S.A. Charman, M.A. Phillips, P.K. Rathod, *J. Med. Chem.* 55 (2012) 7425–7436.
- [9] J.S. Barradas, M.I. Errea, N.B. D'Accorso, C.S. Sepúlveda, E.B. Damonte, *Eur. J. Med. Chem.* 46 (2011) 259–264.
- [10] (a) A. Andreani, M. Granaola, A. Leoni, A. Locatelli, R. Morigi, M. Rambaldi, L. Varoli, D. Lannigahn, J. Smith, D. Scudiero, S. Kondapaka, R.H. Shoemaker, *Eur. J. Med. Chem.* 46 (2011) 4311–4323; (b) A.R. Ali, E.R. El-Bendary, M.A. Ghaly, I.A. Shehata, *Eur. J. Med. Chem.* 75 (2014) 492–500; (c) A. Kamal, D. Dastagiri, M.J. Ramaiah, J.S. Reddy, E.V. Bharathi, Ch. Srinivas, S.N.C.V.L. Pushpavalli, D. Pal, M. Pal-Bhadra, *ChemMedChem* 5 (2010), 1937–147; (d) A. Kamal, G.B. Kumar, V.L. Nayak, V.S. Reddy, A.B. Shaik Rajender, M.K. Reddy, *Med. Chem. Commun.* 6 (2015) 606–612.
- [11] A. Dylong, M. Sowa, W. Goldeman, K. Slepokura, M. Duczmal, A. Wojciechowska, E. Matczak-Jon, *Polyhedron* 75 (2014) 9–21.
- [12] A. Dylong, M. Sowa, W. Goldeman, K. Slepokura, P. Drożdżewski, B. Szponar, E. Matczak-Jon, *J. Coord. Chem.* 68 (2015) 2208–2224.
- [13] F. Palagiano, L. Arenare, E. Luraschi, P. de Caprariis, E. Abignente, M. D'Amico, W. Filippelli, F. Rossi, *Eur. J. Med. Chem.* 30 (1995) 901–909.
- [14] A. Burger, G.E. Ullyot, *J. Org. Chem.* 12 (1947) 342–355.
- [15] S. Laneri, A. Sacchi, M. Galliatelli, F. Arena, E. Luraschi, E. Abignente, W. Filippelli, F. Rossi, *Eur. J. Med. Chem.* 33 (1998) 163–170.
- [16] A. Sacchi, S. Laneri, F. Arena, E. Luraschi, E. Abignente, M. D'Amico, L. Berrino, F. Rossi, *Eur. J. Med. Chem.* 32 (1997) 677–682.
- [17] E. Abignente, F. Arena, P. De Caprariis, *Farm. Ed. Sci.* 31 (1976) 731–737.
- [18] Oxford Diffraction, CRYALSIS/CCD and CRYALSIS/RED Kuma KM4-CCD Software, Oxford Diffraction Ltd., Yarnton, Oxfordshire, England, 2009.
- [19] (a) G.M. Sheldrick, *Acta Crystallogr. Sect. A* 64 (2008) 112–122; (b) G.M. Sheldrick, *Acta Crystallogr. Sect. C* 71 (2015) 3–8.
- [20] K. Brandenburg, DIAMOND, Crystal Impact GbR, Bonn, Germany, 2005.
- [21] S.K. Wolff, D.J. Grimwood, J.J. McKinnon, M.J. Turner, D. Jayatilaka, M.A. Spackman, CRYSTALEXPLORER (Version 3.0), University of Western Australia, 2012.
- [22] M.J. Frisch, G.W. Trucks, H.B. Schlegel, G.E. Scuseria, M.A. Robb, J.R. Cheeseman, G. Scalmani, V. Barone, B. Mennucci, G.A. Petersson, H. Nakatsuji, M. Caricato, X. Li, H.P. Hratchian, A.F. Izmaylov, J. Bloino, G. Zheng, J.L. Sonnenberg, M. Hada, M. Ehara, K. Toyota, R. Fukuda, J. Hasegawa, M. Ishida, T. Nakajima, Y. Honda, O. Kitao, H. Nakai, T. Vreven, J.A. Montgomery Jr., J.E. Peralta, F. Ogliaro, M. Bearpark, J.J. Heyd, E. Brothers, K.N. Kudin, V.N. Staroverov, T. Keith, R. Kobayashi, J. Normand, K. Raghavachari, A. Rendell, J.C. Burant, S.S. Iyengar, J. Tomasi, M. Cossi, N. Rega, J.M. Millam, M. Klene, J.E. Knox, J.B. Cross, V. Bakken, C. Adamo, J. Jaramillo, R. Gomperts, R.E. Stratmann, O. Yazyev, A.J. Austin, R. Cammi, C. Pomelli, J.W. Ochterski, R.L. Martin, K. Morokuma, V.G. Zakrzewski, G.A. Voth, P. Salvador, J.J. Dannenberg, S. Dapprich, A.D. Daniels, O. Farkas, J.B. Foresman, J.V. Ortiz, J. Cioslowski, D.J. Fox, Gaussian 09, Revision D.01, Gaussian, Inc., Wallingford CT, 2013.
- [23] A.D. Becke, *J. Chem. Phys.* 104 (1996) 1040–1046.
- [24] A.D. Hay, W.R. Wadt, *J. Chem. Phys.* 82 (1985) 270–283.
- [25] S.E. Lappi, W.B. Collier, S. Franzen, *J. Phys. Chem. A* 106 (2002) 11446–11455.
- [26] www.chemcraftprog.com.
- [27] <http://cccbdb.nist.gov/vibscalejust.asp>.
- [28] E. Abignente, F. Arena, P. De Caprariis, L. Parente, *Farm. Ed. Sci.* 30 (1975) 815–822.
- [29] E. Abignente, F. Arena, P. De Caprariis, L. Parente, *Farm. Ed. Sci.* 31 (1976) 880–887.
- [30] M.C. Etter, *Acc. Chem. Res.* 23 (1990) 120–126.
- [31] (a) R.E. Rosenfield Jr., R. Parthasarathy, J.D. Dunitz, *J. Am. Chem. Soc.* 99 (1977) 4860–4862; (b) F.W. Heinemann, W. Dölling, H. Hartung, *J. Chem. Crystallogr.* 25 (1995) 463–467.
- [32] T. Steiner, *Angew. Chem. Int. Ed.* 41 (2002) 48–76.